Carbohydrate Polymers 74 (2008) 787–796

Contents lists available at ScienceDirect

Carbohydrate Polymers

journal homepage: www.elsevier.com/locate/carbpol

Resistant glutarate starch from adlay: Preparation and properties

Mi Jung Kim [a], Seung Jun Choi [a], Sang Ick Shin [b], Ma Ri Sohn [a], Chang Joo Lee [a], Yang Kim [a], Wan Il Cho [a], Tae Wha Moon [a,*]

[a] Department of Agricultural Biotechnology, Center for Agricultural Biomaterials, and Research Institute for Agriculture and Life Sciences, Seoul National University, Seoul 151-921, Republic of Korea
[b] Korea Yakult R&D Center, Korea Yakult, Yongin, Gyeonggi-do 446-901, Republic of Korea

ARTICLE INFO

Article history:
Received 30 July 2007
Received in revised form 2 March 2008
Accepted 29 April 2008
Available online 10 May 2008

Keywords:
Adlay starch
Esterification
Glutaric acid
Resistant starch

ABSTRACT

Reaction conditions were optimized to increase the content of resistant starch in adlay starch using esterification with glutaric acid, and the physicochemical properties of the prepared glutarate starches were investigated. Different amounts of glutaric acid (0.1–0.5 g/g starch, dry weight basis) were reacted with adlay starch at various temperatures (70–130 °C) and reaction times (3–9 h). The resistant starch levels increased with increased glutaric acid content, reaction temperature, and reaction time. The color difference was mainly affected by reaction time. The highest resistant starch content (RS 66%) was obtained using conditions of 0.4 g glutaric acid/g starch, 115 °C, and 7.5 h, with a color difference of 10.24. After digestion with α-amylase and amyloglucosidase, the water-soluble fraction of glutarate starch had more oligosaccharides than high-amylose maize starch (RS 43%). FT-IR and solid-state NMR detected carbonyl groups in the glutarate starch, indicating the formation of cross-linkages through esterification. The granular structure of the glutarate starches was not destroyed and they retained birefringence. After heating with an excess of water, the granules kept their shape but lost their birefringence. The glutarate starches had low solubility in both cold and hot water, and the resistant starch contents were unchanged after heating due to the restriction of swelling by cross-linking. The glutarate starches had a similar chain-length distribution to raw starch, indicating that acid hydrolysis took place at branching points in the amorphous region. Furthermore, the glutarate starches possessed a weaker crystalline region, more diverse double helical chains, and lower enthalpy than raw starch.

1. Introduction

In plants, starch is the main carbohydrate reserve and an important ingredient in human nutrition. Nutritionally, starch is classified into rapidly digestible starch, slowly digestible starch, and resistant starch (RS) based on the rate and degree of digestion (Englyst, Kingman, & Cummings, 1992). Resistant starch escapes enzymatic digestion in the small intestine, but in the large intestine microbial flora may ferment some RS. RS displays many of the physiological benefits of dietary fiber, such as calorie reduction, colonic health, increased stool bulk, decreased stool transit time, and generation of volatile free fatty acids (Bird, Brown, & Topping, 2000; Brouns, Kettlitz, & Arrigoni, 2002; Murray et al., 1998; Silvester, Bingham, & Pollock, 1995). RS acts like dietary fiber as it has a probiotic effect on colon microflora, alters lipid metabolism, improves cholesterol metabolism, and reduces the risk of ulcerative colitis; it also reduces the glycemic index of foods (Hoebler, Karinthi, Chiron, Champ, & Barry, 1999).

RS is classified into four categories based on its resistance to digestion. RS1 is physically inaccessible to digestion by entrapment in a non-digestible matrix, RS2 is ungelatinized starch, RS3 is retrograded starch, and RS4 is chemically modified starch (Englyst et al., 1992; Thompson, 2000).

RS4 can be produced by chemical modifications, such as conversion, substitution, or cross-linking, which can prevent its digestion by blocking enzyme access and forming atypical linkages such as 1→2, 1→3, 1→4, and 1→6 linkages (Wurzburg, 1986). Klaushofer, Berghofer, and Steyrer (1978) developed a cross-linked starch using citric acid. Xie and Liu (2004) and Xie, Liu, and Cui (2006) established conditions for the preparation of resistant citrate starch based on the Klaushofer method and studied its physicochemical properties and granular structure. Citrate starches showed no pathological changes as compared to native wheat and corn starches (Klaushofer et al., 1978).

Polyfunctional carboxylic acids (malic, tartaric, citric, malonic, succinic, glutaric, and adipic acids) have been used in the synthesis of hydrogels, and the carboxymethyl starch hydrogels have been rheologically characterized (Seidel et al., 2001).

Coix lachryma-jobi L., commonly known as adlay or Job's tears, is a grass crop widely grown in East Asia. The grain is generally

* Corresponding author. Tel.: +82 2 880 4854; fax: +82 2 873 5095.
E-mail address: twmoon@snu.ac.kr (T.W. Moon).

0144-8617/$ - see front matter © 2008 Elsevier Ltd. All rights reserved.
doi:10.1016/j.carbpol.2008.04.043

spherical, about 5 mm in diameter, and has a hard, shiny dark brown to gray hull. Adlay has long been used as a traditional Oriental medicine, and is also used in baked products, soups, tea, and distilled liquor as flour or whole grain (Arora, 1977). It has been reported that adlay grains may have antitumor activity (Numata, Yamamoto, Moribayashi, & Yamada, 1994) and be effective against viral infection (Hidaka, Kaneda, Amino, & Miyai, 1992). Owing to its perceived nutritional and health value, adlay is increasingly utilized in functional foods and drinks (Li & Corke, 1999). Although adlay grains are high in starch, only a few studies have been done on the physicochemical properties of its starch (Ikawa, Kang, Asaoka, Sakamoto, & Fuwa, 1983; Li & Corke, 1999; Ramirez, 1996a, b; Woo, Yoon, & Kim, 1985). Furthermore, there has been no report on modification of adlay starch for more efficient utilization of adlay in the food industry and exploration of new product development with adlay.

In this study, glutaric acid, a potential food acidulant (Merten & Bachman, 1978), was used as a cross-linking agent. Citric acid has three carboxyl groups that react with hydroxyl groups in the starch chain to form ester bonds; glutaric acid with two carboxyl groups reacts similarly. Nevertheless, due to the difference in number of carboxyl groups, glutarate and citrate starches have different physicochemical and structural properties. We also investigated the physicochemical and structural properties of glutarate starch with a high resistant starch content and a low color difference.

2. Materials and methods

2.1. Preparation of adlay starch

Adlay (*Coix lachryma-jobi* L. var. ma-yuen Stapf) was obtained from Yonchon Nonghyup (Yeoncheon-gun, Gyeonggi-do, Republic of Korea). Adlay starch was isolated using the alkaline steeping method (Wilson, Birmingham, Moon, & Snyder, 1978) with slight modifications. Grains were steeped in excess water for 18 h at room temperature, ground in a blender (707SB, Waring Commercial, Torrington, CT, USA) at full speed for 1 min, and filtered stepwise through 50-, 100-, and 200-mesh sieves. Starch was isolated from the filtrate by centrifugation at 4410*g* for 10 min. The supernatant was discarded, and the top, yellowish layer of protein was removed. This step was repeated until a white starch layer containing no protein was obtained, as determined by ninhydrin reaction of the supernatant. The starch layer was resuspended in distilled water, shaken, and centrifuged as described above. The starch slurry was then neutralized by repeated washing and dried at room temperature.

2.2. Experimental design

A three-factor, five-level central composite design was used to study the effect of each parameter on the RS content and color difference. The independent variables were glutaric acid content (0.1, 0.2, 0.3, 0.4, and 0.5 g/g starch), reaction temperature (70, 85, 100, 115, and 130 °C), and reaction time (3, 4.5, 6, 7.5, and 9 h). The levels of each variable were coded as −2, −1, 0, +1, or +2, as established through preliminary experiments. The dependent variables were the RS content and color difference. A total of 45 experiments with three replicates of one center point, eight factorial points, and six axial points were generated using SAS software (version 9.1; SAS Inc., Cary, NC, USA).

2.3. Preparation of glutarate starch

Glutarate starches were produced using the method of Klaushofer et al. (1978) with modifications. Glutaric acid (Aldrich, St. Louis, MO, USA) was dissolved in water, the pH adjusted to 3.5 with 10 M NaOH, and water added to give a final volume of 10 mL. The glutaric acid solution (10 mL) was mixed with 10 g starch in a stainless-steel bowl and conditioned for 16 h at room temperature. The bowl was then placed in a forced-air oven and dried at 50 °C for 24 h. The mixture was ground and dried in a forced-air oven for 3–9 h at a temperature of 70–130 °C. The dry mixture was washed with 1.5 L of water to remove unreacted glutaric acid, and then air-dried at room temperature and ground. Starch without glutaric acid was used as a control following the same procedure.

2.4. Measurement of resistant starch

Analysis of resistant starch was performed using the Megazyme method (AACC International, 2001). A 100-mg sample was placed in a screw-cap tube, and 4.0 mL of pancreatic α-amylase (10 mg/mL) containing amyloglucosidase (3 U/mL) were added. The tube was incubated with continuous shaking at 37 °C for 16 h. Next, 4.0 mL of ethanol were added, and the solution was stirred on a vortex mixer and centrifuged at 1500*g* for 10 min. The supernatant was decanted and the pellet resuspended in 2 mL of 50% ethanol with vigorous stirring on a vortex mixer. Another 6 mL of 50% ethanol were added to the tube, and the tube was centrifuged at 1500*g* for 10 min. The supernatant was immediately transferred to a new microtube and the suspension/centrifugation step repeated. After centrifugation, the supernatant was collected in a new microtube. The supernatants from the centrifugation of the initial incubation and the subsequent 50% ethanol wash were combined and adjusted to 100 mL with water in a volumetric flask. A 0.1-mL aliquot of this solution was incubated with 3.0 mL of GOPOD reagent at 50 °C for 20 min, and the absorbance was measured at 510 nm against a reagent blank. The non-resistant and resistant starch contents were calculated as follows:

$$\text{Non-resistant starch(g)/100g of sample} = \Delta A \times F/W \times 90$$

where ΔA is the absorbance (reaction) *versus* the reagent blank, F is the conversion factor from absorbance to micrograms (100 μg of glucose/GOPOD absorbance for 100 μg of glucose), and W is the dry weight of the sample (mg).

$$\text{Resistant starch} = \text{Total starch} - \text{Non-resistant starch}$$

2.5. Measurement of color and color difference

The color and color difference were analyzed with a Chroma Meter (CR-300; Minolta, Tokyo, Japan) using the Hunter system, which identifies color using three attributes: L (white = 100, black = 0), a (red = positive, green = negative), and b (yellow = positive, blue = negative). The color difference (ΔE), a measure of the distance in color space between two colors, was determined by comparison to a white standard tile with colorimeter values of $L = 94.7$, $a = 6.7$, and $b = -5.0$, using the following relationship:

$$\Delta E = \sqrt{\Delta L^2 + \Delta a^2 + \Delta b^2}$$

2.6. Fourier transform-infrared spectroscopy (FT-IR)

IR spectra were measured using FT-IR (Nicolet Magna 550 Series II; Midac, Costa Mesa, CA, USA). The spectra were recorded in transmission mode from 4000 to 400 cm (mid-infrared region) at a resolution of 4 cm. Samples were diluted with KBr (1:100, v/v) before acquisition; the background value from pure KBr was acquired before the sample was scanned. The

measured spectra were analyzed using the OMNIC data analysis software.

2.7. Solid-state NMR

CP-MAS ^{13}C NMR spectra were recorded on a DSX-400 (Bruker, Karlsruhe, Germany) equipped with CP-MAS accessories. Dipolar decoupling was systematically used during the acquisition sequence. Samples were spun at 5 kHz at room temperature in a 4-mm rotor with a spectral width of 3.1 kHz. The acquisition time was 35 ms, with 2.2 k time-domain points and a line broadening of 10 Hz. Spectra were analyzed using the high-field resonance of adamantine (29.5 ppm) as a reference.

2.8. High-performance anion exchange chromatography (HPAEC)

Raw starch (10 mg), glutarate starch, and a control were solubilized in 1 M KOH (100 μL) and heated for 5 min. Each solution was neutralized with 1 M HCl (100 μL) and mixed with 800 μL of distilled water, and a 500-μL aliquot of each was mixed with 490 μL of sodium citrate (50 mM, pH 6.0) and 10 μL of isoamylase (Sigma, St. Louis, MO, USA). The mixture was incubated at 40 °C for 16 h in a water bath and boiled for 10 min to stop the reaction.

The debranched chain-length distribution of native and glutarate starches was analyzed using a HPAEC system (Dionex-300; Dionex, Sunnyvale, CA, USA) with a pulsed amperometric detector (PAD; ED-40; Dionex). All samples were filtered through a 0.45-μm filter, and an aliquot was injected onto a CarboPac™ PA-1 (250 × 4 mm; Dionex). After equilibration of the column with 150 mM NaOH, the sample was eluted with varying gradients of 600 mM sodium acetate in 150 mM NaOH at a flow rate of 1 mL/min. The sodium acetate gradients used were linear gradients of 10–30% for 0–10 min, 30–40% for 10–16 min, 40–50% for 16–27 min, 50–60% for 27–44 min, and 60–64% for 44–60 min.

2.9. X-ray diffractometry

X-ray diffraction analysis was performed with a diffractometer (D5005; Bruker, Karlsruhe, Germany) operating at 30 kV and 40 mA with Cu Kα radiation of 0.154 nm (nickel filter). The sample was scanned through the 2θ range from 3 to 30°.

2.10. Differential scanning calorimetry (DSC)

Thermal properties were investigated using a differential scanning calorimeter (DSC 120, Seiko, Chiba, Japan). Indium was used as the calibration standard. A 3-mg starch sample was placed in a Seiko high-pressure stainless-steel pan, and 12 mg of distilled water were added. The pan was sealed and kept at room temperature for 3 h. Distilled water was used as a reference. The sample pan was heated from 30 to 130 °C at 5 °C/min.

2.11. Cold- and hot-water solubility and swelling power

The cold-water solubility (CWS) of the glutarate starch was measured by the method of Schoch (1964) with slight modifications. Starch (25 mg) was added to a 50-mL centrifuge cell containing 25 mL of distilled water at 25 °C, and the sample was stirred for 15 min. Next, the suspension was centrifuged at 1500*g*, and the total sugar content in the supernatant was measured using the phenol-sulfuric acid method (Dubois, Gilles, Hamilton, Rebers, & Smith, 1956). To measure the hot-water solubility (HWS) and swelling power, 20 mg of starch were added to a 50-mL centrifuge cell containing 25 mL of distilled water. The centrifuge cell was heated in a water bath (80 °C) for 15 min with intermittent vortexing, and then centrifuged at 1500*g* for 20 min. The HWS and swelling power were determined as follows: HWS = (weight of dissolved solids in supernatant/weight of dry sample solids in original sample) × 100; swelling power = weight of sediment/weight of dry sample solids.

2.12. Light microscopy

Light microscopy was performed using a CSB-HP3 light microscope (Sam Won Scientific, Seoul, South Korea) equipped with a polarizer. A digital camera (Nikon, Tokyo, Japan) was used for image capture. All samples were dispersed in glycerol on a microscope slide.

2.13. Scanning electron microscopy (SEM)

A dry, finely ground sample was placed on double-sided Scotch tape mounted on an aluminum specimen holder and coated with a thin film of gold under vacuum. Samples were imaged on a Jeol scanning electron microscope at 30 kV (JSM 5410LV; Jeol, Tokyo, Japan).

3. Results and discussion

3.1. Establishment of optimal conditions

The RS content and color difference results are shown in Table 1. Regression analysis showed that the RS content and color difference were mainly influenced by the amount of glutaric acid and the reaction temperature, followed by the reaction time. The RS content increased with increasing glutaric acid content, reaction temperature, and reaction time. An increase in the RS content with these parameters was expected, as glutaric acid, serving as a cross-linking agent between starch chains, as well as the reaction temperature and time conditions used in the experiment, promote esterification. Similar results were also observed for the color difference, which was mainly affected by the reaction temperature. At longer reaction times, the color difference increased with the reaction temperature, but at shorter reaction times, the color difference was small at a reaction temperature of approximately 80 °C.

The conditions necessary for the preparation of glutarate starch with a high RS content and low color difference are of interest. The highest RS content was in samples 8 (0.4 g, 115 °C, 7.5 h, with 66% RS) and 13 (0.3 g, 130 °C, 6 h, with 65% RS), with color differences of 10.24 and 20.06, respectively. Therefore, satisfactory conditions for the preparation of glutarate starch were glutaric acid 0.4 g/g starch, a reaction temperature of 115 °C, and a reaction time of 7.5 h. These conditions differ from previously reported conditions for the preparation of citrate starch, especially in the temperature (0.4 g of citric acid/g corn starch, 140 °C, 7 h; Xie & Liu, 2004). The organic acid influences the reaction temperature because the melting point of citric acid (153 °C) is higher than that of glutaric acid (98 °C). When citric acid and waxy corn starch were used to prepare cross-linked starch, the RS content was 87.5%, higher than that of glutarate adlay starch. However, when citric acid was reacted with normal corn starch at 120 °C, the RS content was 37.5%. Therefore, for the preparation of cross-linked starch, glutaric acid is more energy-efficient than citric acid.

3.2. Structural characteristics of glutarate adlay starch

3.2.1. Identification of cross-linking with glutaric acid

The characteristic functional groups in the prepared blends of glutarate starch were confirmed by FT-IR spectroscopy. IR spectra of the glutarate starches showed peaks typical of a starch backbone (Fig. 1). A broad peak appeared in the range of 3000–3500 cm, indi-

Table 1
Resistant starch contents and color differences of glutarate adlay starches

	Acid content (g/g)	Temperature (°C)	Time (h)	RS content (%)	ΔE
Raw starch				17.93 ± 1.48	7.39 ± 0.02
Control	0	115	7.5	11.40 ± 1.08	7.23 ± 0.02
1	0.2 (−1)	85 (−1)	4.5 (−1)	14.92 ± 2.33	7.91 ± 0.27
2	0.2 (−1)	85 (−1)	7.5 (1)	13.66 ± 2.44	7.85 ± 0.21
3	0.2 (−1)	115 (1)	4.5 (−1)	25.42 ± 3.30	7.55 ± 0.21
4	0.2 (−1)	115 (1)	7.5 (1)	30.28 ± 3.51	7.38 ± 0.18
5	0.4 (1)	85 (−1)	4.5 (−1)	22.48 ± 5.46	7.84 ± 0.20
6	0.4 (1)	85 (−1)	7.5 (1)	23.52 ± 3.11	7.82 ± 0.12
7	0.4 (1)	115 (1)	4.5 (−1)	51.58 ± 1.99	7.53 ± 0.28
8	0.4 (1)	115 (1)	7.5 (1)	66.38 ± 3.24	10.24 ± 0.50
9	0.3 (0)	100 (0)	6 (0)	28.47 ± 2.35	7.74 ± 0.20
10	0.1 (−2)	100 (0)	6 (0)	13.37 ± 3.97	7.15 ± 1.12
11	0.5 (2)	100 (0)	6 (0)	44.55 ± 0.52	7.38 ± 0.04
12	0.3 (0)	70 (−2)	6 (0)	12.82 ± 0.37	7.76 ± 0.02
13	0.3 (0)	130 (2)	6 (0)	65.44 ± 3.85	20.06 ± 2.22
14	0.3 (0)	100 (0)	3 (−2)	21.68 ± 2.96	6.94 ± 1.27
15	0.3 (0)	100 (0)	9 (2)	35.7 ± 2.63	6.61 ± 1.50

cating the presence of starch hydroxyl groups. The spectra depict C–H stretching at 2930 cm and prominent C–O–C stretching of the glycosidic bonds at 1163 cm, typical of starch (Bajpai & Shrivastava, 2005). Compared to native starch, an additional absorption band appeared at 1730 cm in the glutarate starch spectrum, which could be ascribed to the carbonyl absorption band (Saikia, Ali, Goswami, & Ghosh, 1995). The peak intensity was greater for sample 8 (RS 30%) than for sample 4 (RS 66%), suggesting that the high RS content results from esterification.

High resolution solid-state ^{13}C NMR spectra of native starch and control and glutarate starches were obtained using cross-polarization, magic angle spinning, and high-power dipolar decoupling (Fig. 2). Intensity in the regions of 90–110, 67–90, and 58–67 ppm was assigned to the C-1, C-2, -3, -4, -5, and C-6 sites, respectively (Gidley & Bociek, 1985). The A type indicates three peaks at 100.4, 99.2, and 98.2 ppm, and the B type shows two peaks at 100.0 and 99.2 ppm. All of the starch samples had three peaks, indicating the A type. For the glutarate starches, the new peaks at 173 and 32 ppm were assigned as a carbonyl group and a methylene group, respectively, revealing cross-linking between starch chains by esterification (Grote & Heinze, 2005). The intensities of these peaks were also greater for sample 8 (RS 66%) than for sample 4 (30%).

3.2.2. Soluble oligomers after digestion

After degradation of starch with pancreatic α-amylase and amyloglucosidase, high-amylose maize starch (used as the RS control at 43%), raw starch, and sample 11 of glutarate starch with an RS content (45%) similar to that of the control were analyzed for soluble oligomers with HPAEC-PAD (Fig. 3). Glutarate starch had more soluble oligomers resistant to the digestive enzymes than raw starch. These results suggest that glutarate starches have glycosidic linkages that are not hydrolyzed by the digestive enzymes. The HPAEC-PAD chromatograms showed that glutarate starch had some soluble oligomers, the peaks between G4 and G5, and between G5 and G6, that RS control did not have. The new peaks did not come from the cross-linkages formed with glutaric acid because most of the cross-linkages were lost during the solubilization process in 1 M KOH. The new peaks could come from atypical linkages, which could not be hydrolyzed by debranching enzyme. Atypical linkages, having 1,6-β-D glucosidic bond or intermolecular bond, could be formed during drying at high temperature and predrying under acidic conditions, although these conditions were not exactly the same as those for pyroconversion (Wurzburg, 1986).

3.2.3. Chain-length distribution

After dissolving the cross-links in glutarate starches by saponification with KOH, the chain-length distributions were analyzed (Fig. 4). All of the samples were debranched by isoamylase. Before the analysis of the chain-length distributions, we determined if the cross-linkages in glutarate starches were lost at alkaline pH using

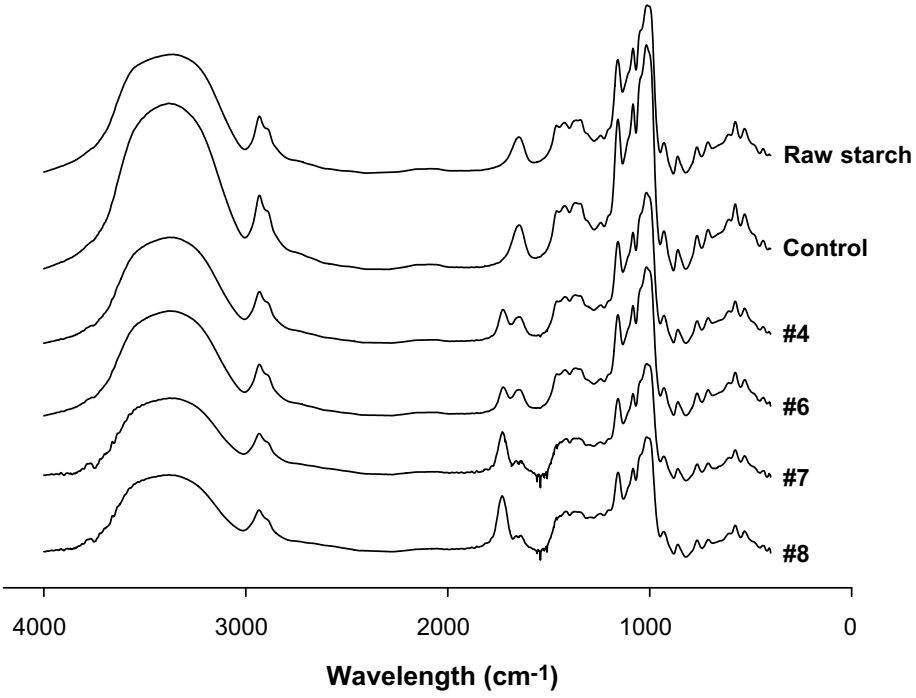

Fig. 1. FT-IR spectra of raw starch, control, and glutarate starch samples 4 (0.2 g, 115 °C, 7.5 h, RS 30%), 6 (0.4 g, 85 °C, 7.5 h, RS 24%), 7 (0.4 g, 115 °C, 4.5 h, RS 52%), and 8 (0.4 g, 115 °C, 7.5 h, RS 66%).

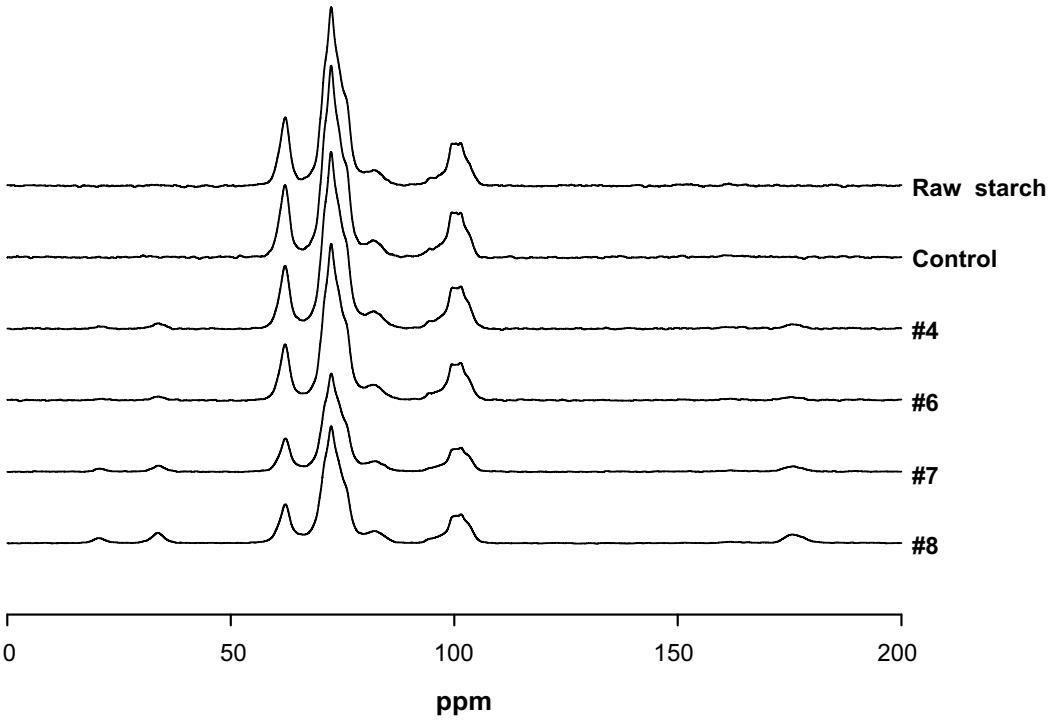

Fig. 2. ^{13}C NMR spectra of raw starch, control, and glutarate starch samples 4 (0.2 g, 115 °C, 7.5 h, RS 30%), 6 (0.4 g, 85 °C, 7.5 h, RS 24%), 7 (0.4 g, 115 °C, 4.5 h, RS 52%), and 8 (0.4 g, 115 °C, 7.5 h, RS 66%).

FT-IR. We confirmed that most of the cross-linkages in glutarate starch were hydrolyzed at alkaline pH (data not shown). The chain-length distributions of glutarate starches were similar to those of raw and control starches, indicating that acid hydrolysis preferentially occurred in the amorphous region. This result agrees with a previous report on the hydrolysis of potato starch with 2.2 N HCl, in which rapid hydrolysis occurred in the amorphous regions of the granules at an early step, followed by gradual hydrolysis in the crystalline region during a second step (Robin, Mercier, Charbonniere, & Guilbot, 1974). In our study, acid hydrolysis mainly took place for a short time during the conditioning step; therefore, most of the acid hydrolysis occurred in the amorphous region,

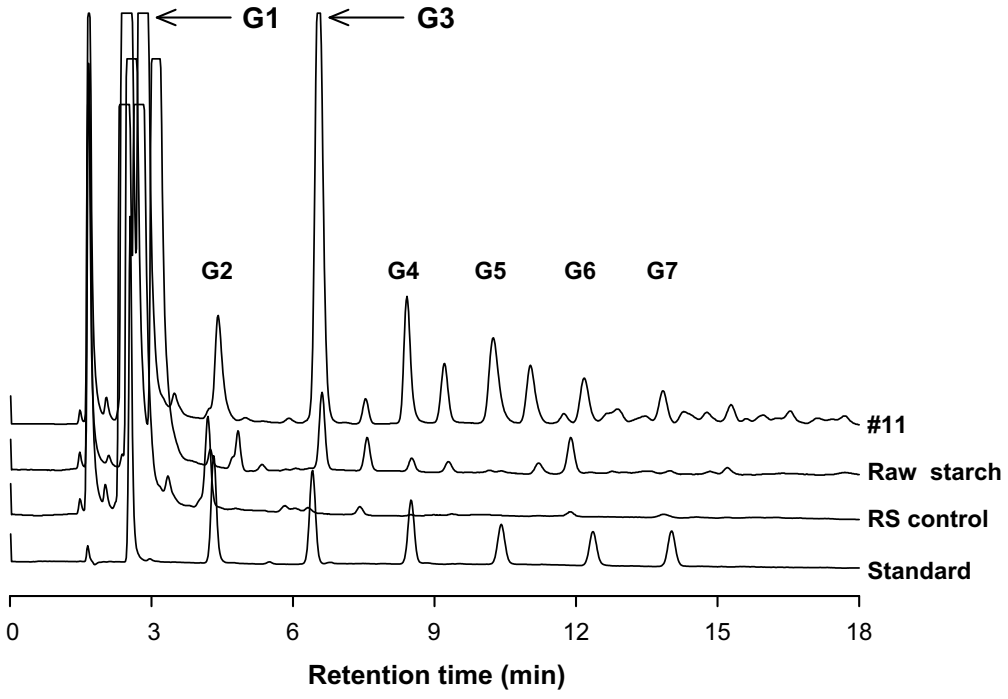

Fig. 3. Soluble oligomers after digestion of sample 11 (0.3 g, 100 °C, 6 h, RS 45%) and control high-amylose maize starch (RS 43%).

especially at branching points, as suggested by Mussulman and Wagoner (1968) and Robin et al. (1974).

3.2.4. X-ray diffraction

X-ray diffractograms of raw starch, control, and the glutarate starches are shown in Fig. 5. Raw adlay starch displayed peaks at 5.5°, 15°, 17°, 18°, and 23°. Zobel (1964) and Hizukuri, Abe, and Hanashiro (2006) reported that X-ray diffraction peaks at 15°, 17°, 18° and 23°, and at 5.5°, 15°, 17°, 22°, and 24° are characteristics of A- and B-type starches, respectively. Adlay starch showed an X-ray diffractogram similar to A-type, but it was not a typical A-type because the weak peak at 5.5°, which is characteristic of B-type pattern, was observed in its X-ray diffractogram. During preparation of the glutarate starch, the X-ray diffraction patterns of glutarate starch were not changed compared to raw starch, although the split peak of 17° and 18° was not observed clearly in sample 8. The crystal structure could be affected by acid hydrolysis with heat treatment (Biliaderis, Grant, & Vose, 1981). The relative crystallinities of the glutarate starch samples 4, 6, 7, and 8 were about 55.4%, 54.7%, 47.0%, and 41.0%, respectively, which were lower than that of raw starch because the crystalline region was disrupted to some extent by acid and heat treatment during preparation. The peak intensities of the glutarate starches were also lower than that of raw starch. Similar results to our findings have been reported by Xie et al. (2006). They explained that the smaller crystalline peaks of citrate starches could be due to the disruption of the crystalline structure of granules by a concentrated solution of citric acid penetrating the starch granules through channels and cavities.

3.2.5. Thermal properties

The onset temperature (T_o), peak temperature (T_p), and conclusion temperature (T_c) of the gelatinization of glutarate starch were lower than those of raw starch or the control (Table 2). This result suggested that the internal crystalline structure of the glutarate starch was more easily destroyed at a lower temperature than raw starch or the control. Glutarate starch samples with a higher RS content (sample 8) showed a much lower gelatinization temperature than those with lower RS levels. Glutarate starches showed a broader gelatinization temperature range, $T_c - T_o$, than raw starch or the control. This implies a more heterogeneous structure, reflecting disordering of the starch fractions and variations in the crystallite shape, crystallite size, degree of crystal perfection, and type of starch chain intertwining (linear–linear, linear–branch, or branch–branch), and producing double helical chains of starch crystallites (Hoover & Manuel, 1996; Jayakody & Hoover, 2002). Glutarate starches showed a relatively smaller endotherm values (ΔH) than those of raw starch or the control. This lower enthalpy indicates that the molecular (double helical) and crystalline orders were disrupted during preparation of the glutarate starch (Cooke & Gidley, 1992). The reduced enthalpy could be ascribed to the preparation conditions used for glutarate starch, especially the acid content.

The T_o, T_p, and T_c of glutarate starches were lower than raw starch and the control, but the X-ray diffraction patterns of glutarate starches were similar to those of raw starch and the control. These results suggested that the crystalline structure of granules was disrupted by penetration of glutaric acid into the starch granules through channels and cavities. If most of the crystallites were disrupted, there had to be no crystalline peaks in the X-ray diffractograms of glutarate starches. However, the crystalline peaks were observed in the X-ray diffractograms of glutarate starches, suggesting that the original crystallites located in starch granules were disrupted and those disrupted crystallites were recrystallized during preparation of the glutarate starches. The decreased ΔH and lower T_o, T_p, and T_c were easily observed in retrograded starches. The crystallites formed during preparation were smaller than original crystallites because smaller crystallites were less stable and melted at lower temperature than larger crystallites (Jenkins & Donald, 1997).

3.3. Physicochemical properties of glutarate adlay starch

3.3.1. Cold-water solubility

Table 3 shows the CWSs of starch samples. All samples had very low solubilities, which could be attributed to the semicrystalline

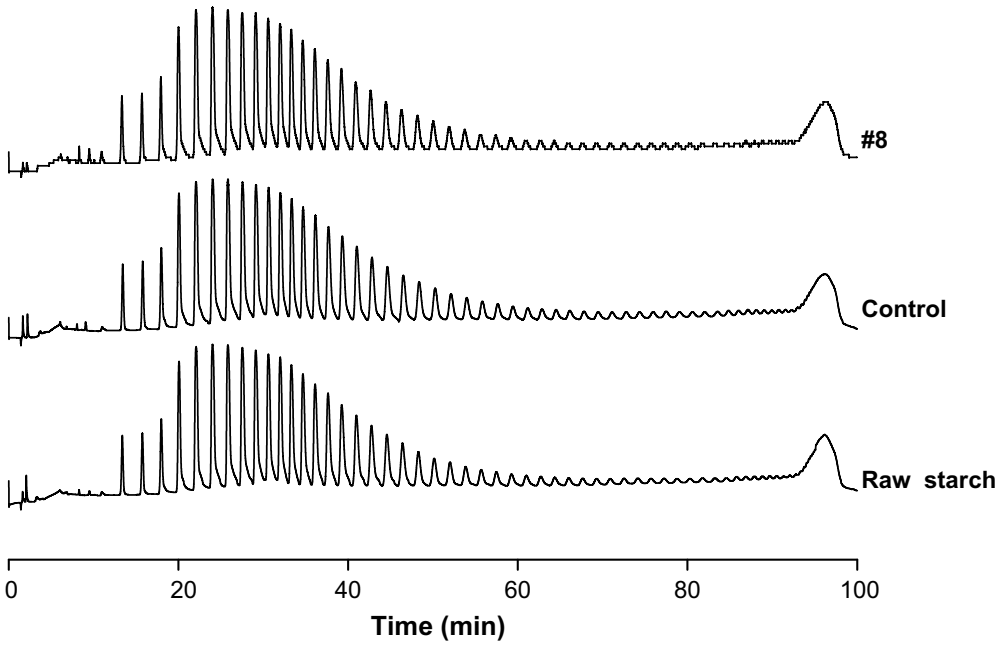

Fig. 4. Chain-length distributions of raw starch, control, and glutarate starch sample 8 (0.4 g, 115 °C, 7.5 h, RS 66%).

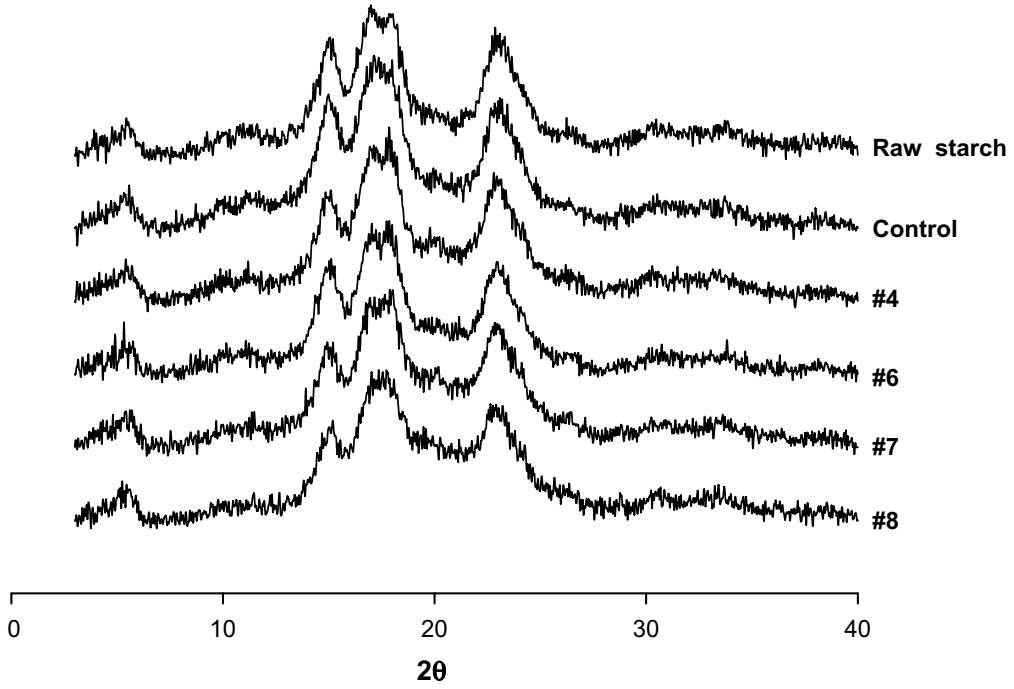

Fig. 5. X-ray diffractograms of raw starch, control, and glutarate starch samples 4 (0.2 g, 115 °C, 7.5 h, RS 30%), 6 (0.4 g, 85 °C, 7.5 h, RS 24%), 7 (0.4 g, 115 °C, 4.5 h, RS 52%), and 8 (0.4 g, 115 °C, 7.5 h, RS 66%).

Table 2
Gelatinization parameters of raw starch, control, and glutarate starches

	T_o	T_p	T_c	$T_c - T_o$	ΔH
Raw starch	61.4 ± 0.5	73.8 ± 0.1	83.3 ± 0.2	21.9 ± 0.6	14.1 ± 0.1
Control	60.0 ± 0.8	71.3 ± 2.5	82.6 ± 0.2	22.6 ± 0.8	13.3 ± 0.5
Sample 4 (0.2 g, 105 °C, 7.5 h, RS 30%)	49.9 ± 1.3	65.6 ± 2.5	73.8 ± 0.5	23.9 ± 1.3	9.5 ± 0.7
Sample 7 (0.4 g, 105 °C, 4.5 h, RS 52%)	48.8 ± 0.5	60.5 ± 0.4	73.1 ± 0.0	26.3 ± 0.5	8.0 ± 0.3
Sample 8 (0.4 g, 105 °C, 7.5 h, RS 66%)	46.0 ± 0.7	61.9 ± 0.1	73.9 ± 0.2	26.8 ± 0.7	5.7 ± 0.4

Table 3
Solubility and swelling power of raw starch, control, and glutarate adlay starches

	Solubility (%)		Swelling power (g/g)
	25 °C	80 °C	
Raw starch	0.24 ± 0.01	82.26 ± 2.67	—
Control	0.12 ± 0.01	81.23 ± 1.84	—
Sample 4 (0.2 g, 105 °C, 7.5 h, 30%)	0.17 ± 0.04	1.52 ± 0.13	7.39 ± 0.38
Sample 6 (0.4 g, 75 °C, 7.5 h, 24%)	0.19 ± 0.06	1.25 ± 0.40	8.12 ± 0.26
Sample 7 (0.4 g, 105 °C, 4.5 h, 52%)	0.21 ± 0.04	0.71 ± 0.31	5.57 ± 0.22
Sample 8 (0.4 g, 105 °C, 7.5 h, 66%)	0.64 ± 0.14	0.88 ± 0.30	5.03 ± 0.20

structure of the starch granule and the hydrogen bonds formed between hydroxyl groups in the starch polymers (Eliasson & Gudmundsson, 2006).

3.3.2. Hot-water solubility

The HWSs of raw starch and the control, determined at 80 °C, were much higher than the respective CWS values, whereas the HWSs of glutarate starches were slightly higher than the CWS (Table 3). The solubility of raw starch increased with the temperature. Granules of glutarate starch held together by cross-links showed reduced swelling and became less soluble in hot water. This reduced swelling could affect the access of the digestive enzymes and their hydrolytic activity.

3.3.3. Swelling power

As the RS content increased, the swelling power of the glutarate starches decreased (Table 3). Because granules of raw adlay starch and the control ruptured at 80 °C, their swelling powers were not determined. This result suggests that cross-linking of internal chains of starch occurred, causing restricted swelling of the granules. This result is in accordance with the low HWS of glutarate starches. Similar results have been reported by Xie et al. (2006), in that the pasting curve of citrate starch was flat and citrate starch with a higher RS content absorbed less water.

3.3.4. Light microscopy

Fig. 6 shows light photomicrographs of glutarate starch before and after heating. Before heating, raw starch, the control, and glutarate starches had intact granules and exhibited birefringence. After heating with excess water, the granules of native starch and the control ruptured. However, the glutarate starch granules did not rupture, even though they swelled during heating, but the birefringence was lost. This result differs from that of a previous study (Xie et al., 2006) that reported a complete loss of birefringence in waxy corn starch citrate, indicating that waxy corn starch has fragile granules that were easily disrupted during citric acid modification. Possible causes of this discrepancy are the dif-

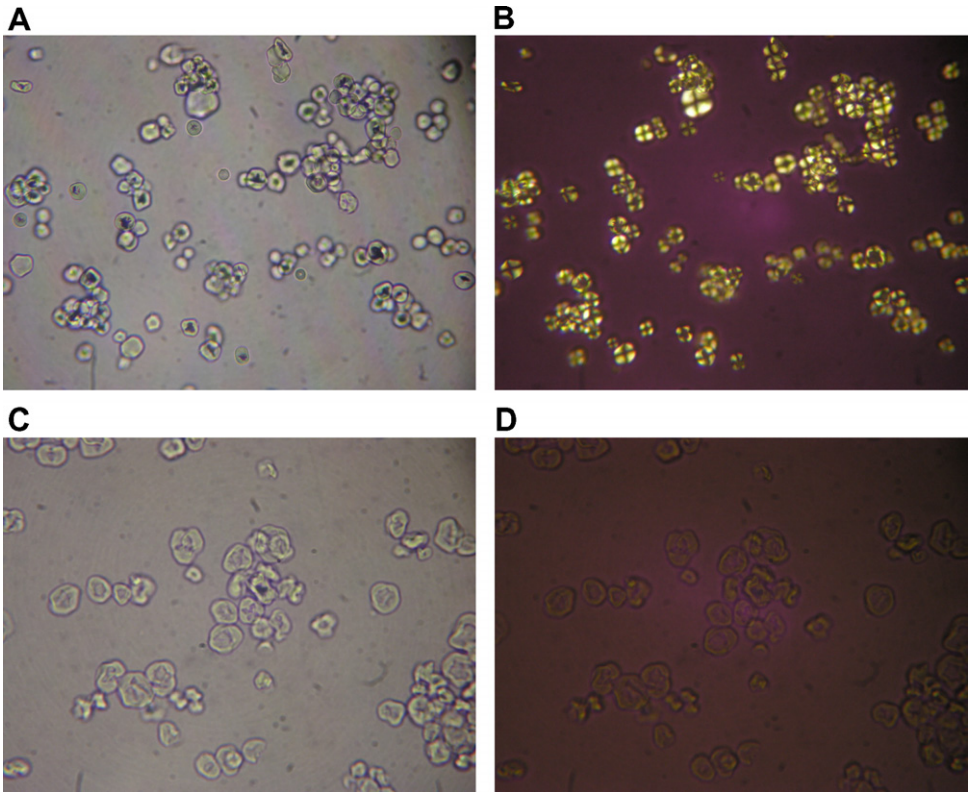

Fig. 6. Light micrographs of glutarate starch (0.4 g, 115 °C, 7.5 h, RS 66%) before and after heating. (A and B) Before heating; (C and D) after heating; (B and D) under polarized light.

ferent botanical origins of the starches, the degree of substitution, the type of organic acid, or the preparation conditions, especially reaction temperature. In this study, the preparation of glutarate adlay starches was carried out at temperatures ranging from 70 to 130 °C, whereas Xie et al. (2006) prepared citrate waxy corn starch at 140 °C.

The effect on the granules of heating with excess water was similar to previous findings. Granules of citrate starches prepared from normal, waxy, and high-amylose corn starches were not collapsed or disrupted during heating (Xie et al., 2006). During heating with excess water, cross-linkage between the starch chains caused the formation of a hard crust and prevented starch granules from further swelling and subsequent destruction. However, heating caused a loss of the "Maltese Cross" pattern due to the melting of starch crystallites.

3.3.5. Scanning electron microscopy

Fig. 7 shows SEM photomicrographs of glutarate starches before and after heating and digestion. Control starch granules are displayed because they show a similar shape to raw adlay starch. Glutarate starch granules also had shapes similar to that of the control, but some granules were partially fragmented. However, after heating at 100 °C for 20 min, some of the glutarate starch granules became doughnut-shaped. Raw starch and the control were gelatinized by heating, and the starch granules became swollen and disrupted. However, glutarate starches either did not swell or showed less swelling than raw starch or the control. Although some glutarate starch granules appeared round or angular in shape after digestion with an α-amylase-amyloglucosidase mixture for 16 h, many of the granules lost their granular shapes and cohered with other granules, whether or not they were heated before digestion. Xie et al. (2006) utilized SEM to observe citrate corn starches and reported that the granules became doughnut-shaped when treated with citric acid. They concluded that the doughnut-shaped granules were due to granular swelling in a concentrated solution of citric acid early in the reaction, with collapse occurring during cooling. However, in our study, doughnut-shaped granules were common in the glutarate starch after heating. These results suggest that the adlay starch granules are well organized and more resistant to swelling in concentrated acid solution. However, in extreme conditions, such as cooking at 100 °C for 20 min, swelling occurs in glutarate starch and the organized structure of the granules partially collapses. The cross-linkage between starch chains explains why the glutarate starch granules were not completely disrupted after cooking.

3.3.6. Thermal stability of glutarate starch

After heating with excess water, the RS content of the glutarate starches was determined (Table 4). The glutarate starch levels were similar before and after heating, as reported by Xie and Liu (2004) for citrate corn starch. They suggested that citrate starch with a higher amylopectin content is more thermally stable than citrate starch with a lower amylopectin content, and that cross-linking with citric acid could restrict the swelling of starch granules in hot water. Digestive enzymes cannot easily access the interior of the starch granules (Tester, Karkalas, & Qi, 2004), and therefore are less likely to hydrolyze the cross-linked starch units.

4. Conclusion

Glutarate starches with RS contents ranging from 13.5 to 66.5% were prepared from adlay starch. The optimal reaction conditions for the formation of glutarate adlay starch with the highest RS content were 0.4 g glutaric acid/g starch, a reaction temperature of

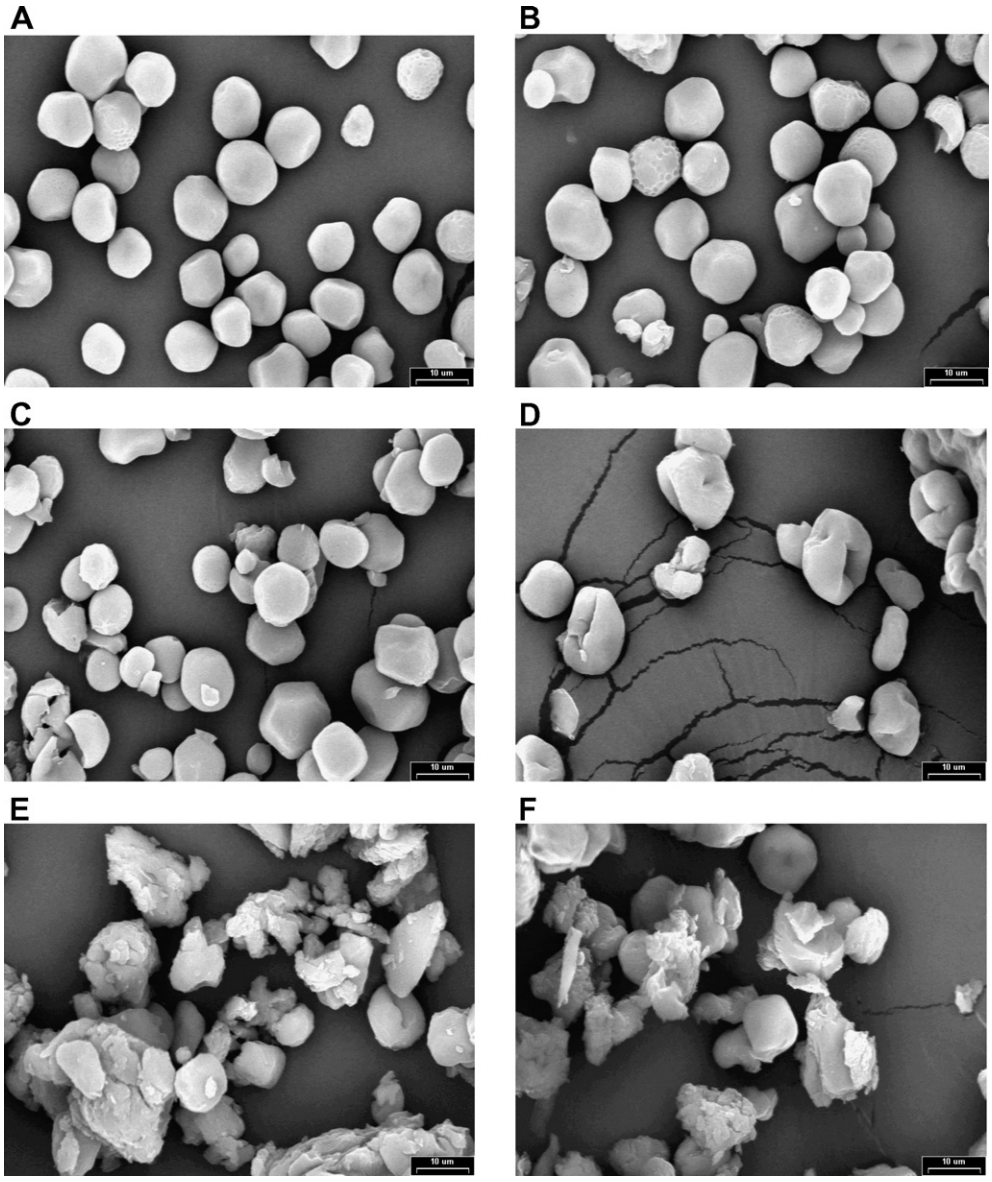

Fig. 7. Scanning electron micrographs of raw adlay starch, control, and glutarate starch before and after heating and digestion. (A) Raw adlay starch; (B) control; (C) 0.4 g, 115 °C, 7.5 h, RS 66%, before heating; (D) 0.4 g, 115 °C, 7.5 h, RS 66%, after heating; (E) 0.4 g, 115 °C, 7.5 h, RS 66%, digested without heating; (F) 0.4 g, 115 °C, 7.5 h, RS 66%, digested after heating.

Table 4
Resistant starch contents of glutarate starches before and after heat treatment

	Resistant starch content (%)	
	Before heating	After heating
Raw starch	17.93 ± 1.48	5.71 ± 2.02
Control	11.40 ± 1.08	6.06 ± 2.73
Sample 4 (0.2 g, 105 °C, 7.5 h, 30%)	30.28 ± 3.51	31.80 ± 2.68
Sample 6 (0.4 g, 75 °C, 7.5 h, 24%)	23.52 ± 3.11	26.69 ± 2.72
Sample 7 (0.4 g, 105 °C, 4.5 h, 52%)	51.58 ± 1.99	51.45 ± 3.52
Sample 8 (0.4 g, 105 °C, 7.5 h, 66%)	66.38 ± 3.24	67.81 ± 4.43

115 °C, and a reaction time of 7.5 h. Glutarate starches had similar chain-length distributions to raw adlay starch and the control. Glutarate starches with lower crystallinity than raw starch had a similar RS content before and after heating with excess water. This glutarate starch could be utilized to enhance the textural properties and health benefits of low-moisture products, such as crackers and cookies, due to its low solubility and digestibility and heat stability.

Acknowledgements

This work was supported by the Korea Research Foundation Grant funded by the Korea Government (MOEHRD, Basic Research Promotion Fund) (KRF-2006-005-J04703) and by the Technology Development Program for Agriculture and Forestry, Ministry of Agriculture and Forestry, Republic of Korea.

References

AACC International. (2001). AACC Report: The definition of dietary fiber. *Cereal Foods World, 46*, 112–126.
Arora, R. K. (1977). Job's tears (*Coix lachryma-jobi* L.)—A minor food and fodder crops of northeastern India. *Economic Botany, 31*, 358–366.
Bajpai, A. K., & Shrivastava, J. (2005). *In vitro* enzymatic degradation kinetics of polymeric blends of crosslinked starch and carboxymethyl cellulose. *Polymer International, 54*, 1524–1536.
Biliaderis, C. G., Grant, D. R., & Vose, J. R. (1981). Structural characterization of legume starches. II. Studies on acid-treated starches. *Cereal Chemistry, 58*, 502–507.

Bird, A. R., Brown, I. L., & Topping, D. L. (2000). Starches, resistant starches, the gut microflora and human health. *Current Issues in Intestinal Microbiology, 1*, 25–37.

Brouns, F., Kettlitz, B., & Arrigoni, E. (2002). Resistant starch and the butyrate revolution. *Trends in Food Science and Technology, 13*, 251–261.

Cooke, D., & Gidley, M. J. (1992). Loss of crystallinity and molecular order during starch gelatinization: Origin of the enthalpic transition. *Carbohydrate Research, 227*, 103–112.

Dubois, M., Gilles, K. A., Hamilton, J. K., Rebers, P. A., & Smith, F. (1956). Colorimetric method for determination of sugars and related substances. *Analytical Chemistry, 28*, 350–356.

Eliasson, A.-C., & Gudmundsson, M. (2006). Starch: Physicochemical and functional aspects. In A.-C. Eliasson (Ed.), *Carbohydrates in food* (2nd ed., pp. 391–469). Boca Raton, FL: CRC Press.

Englyst, H. N., Kingman, S. M., & Cummings, J. H. (1992). Classification and measurement of nutritionally important starch fractions. *European Journal of Clinical Nutrition, 46*, S30–S50.

Gidley, M. J., & Bociek, S. M. (1985). Molecular organization in starches: a ^{13} C CP/MAS NMR study. *Journal of the American Chemical Society, 107*, 7040–7044.

Grote, C., & Heinze, T. (2005). Starch derivatives of high degree of functionalization 11: Studies on alternative acylation of starch with long-chain fatty acids homogeneously in *N*,*N*-dimethyl acetamide/LiCl. *Cellulose, 12*, 435–444.

Hidaka, Y., Kaneda, T., Amino, N., & Miyai, K. (1992). Chinese medicine, coix seeds increase peripheral cytotoxic T and NK cells. *Biotherapy, 5*, 201–203.

Hizukuri, S., Abe, J.-I., & Hanashiro, I. (2006). Starch: Analytical aspects. In A.-C. Eliasson (Ed.), *Carbohydrates in food* (2nd ed., pp. 305–390). Boca Raton, FL: CRC Press.

Hoover, R., & Manuel, H. (1996). The effect of heat-moisture treatment on the structure and physicochemical properties of normal maize, waxy maize, dull waxy and amylomaize V starches. *Journal of Cereal Science, 23*, 153–162.

Hoebler, C., Karinthi, A., Chiron, H., Champ, M., & Barry, J. L. (1999). Bioavailability of starch in bread rich in amylose: Metabolic responses in healthy subjects and starch structure. *European Journal of Clinical Nutrition, 53*, 360–366.

Ikawa, Y., Kang, M. Y., Asaoka, M., Sakamoto, S., & Fuwa, H. (1983). Some properties of starches of Job's tears. *Journal of the Japanese Society of Starch Science, 30*, 5–12.

Jayakody, L., & Hoover, R. (2002). The effect of lintnerization on cereal starch granules. *Food Research International, 35*, 665–680.

Jenkins, P. J., & Donald, A. M. (1997). Breakdown of crystal structure in potato starch during gelatinization. *Journal of Applied Polymer Science, 66*, 225–232.

Klaushofer, H., Berghofer, E., & Steyrer, W. (1978). Stärkecitrate–Produktion und anwendungstechnische Eigenschaften. *Starch/Stärke, 30*, 47–55.

Li, J., & Corke, H. (1999). Physicochemical properties of normal and waxy Job's tears (*Coix lachryma-jobi* L.) starch. *Cereal Chemistry, 76*, 413–416.

Merten, H. L., & Bachman, G. L. (1978). Glutaric acid: A potential food acidulant. *Journal of Food Science, 41*, 463–464.

Murray, S. M., Patil, A. R., Fahey, G. C., Jr., Merchen, N. R., Wolf, B. W., Lai, C. S., et al. (1998). Apparent digestibility of a debranched amylopectin-lipid complex and resistant starch incorporated into enteral formulas fed to ileal-cannulated dogs. *Journal of Nutrition, 128*, 2032–2035.

Mussulman, W. C., & Wagoner, J. A. (1968). Electron microscopy of unmodified and acid-modified corn starches. *Cereal Chemistry, 45*, 162–171.

Numata, M., Yamamoto, A., Moribayashi, A., & Yamada, H. (1994). Antitumor components isolated from the Chinese herbal medicine *Coix lachryma-jobi*. *Planta Medica, 60*, 356–359.

Ramirez, J. L. (1996a). Chracterization of Job's tears starch. I. Extraction and physical properties of the starch granules. *Alimentaria, 276*, 97–100.

Ramirez, J. L. (1996b). Characterization of Job's tears starch. II. Pasting characteristics. *Alimentaria, 276*, 97–100.

Robin, J. P., Mercier, C., Charbonniere, R., & Guilbot, A. (1974). Lintnerized starches. Gel filtration and enzymatic studies of insoluble residues from prolonged acid treatment of potato starch. *Cereal Chemistry, 51*, 389–407.

Saikia, C. N., Ali, F., Goswami, T., & Ghosh, A. C. (1995). Esterification of high α-cellulose extracted from *Hibiscus cannabinus* L. *Industrial Crops and Products, 4*, 233–239.

Schoch, T. J. (1964). Swelling power and solubility of granular starches. In R. L. Whistler (Ed.), *Methods in carbohydrate chemistry, Vol. 4. Starch* (pp. 106–108). New York: Academic Press.

Seidel, C., Kuliche, W. M., Heb, C., Hartmann, B., Lechner, M. D., & Lazik, W. (2001). Influence of the cross-linking agent on the gel structure of starch derivatives. *Starch/Stärke, 53*, 305–310.

Silvester, C., Bingham, S., & Pollock, J. (1995). Ileal recovery of starch from whole diets containing resistant starch measured in vitro and fermentation of ileal effluent. *American Journal of Clinical Nutrition, 62*, 403–413.

Tester, R. F., Karkalas, J., & Qi, X. (2004). Starch structure and digestibility: Enzyme-substrate relationship. *World's Poultry Science Journal, 60*, 186–195.

Thompson, D. B. (2000). Strategies for the manufacture of resistant starch. *Trends in Food Science and Technology, 11*, 245–253.

Wilson, L. A., Birmingham, V. A., Moon, D. P., & Snyder, H. E. (1978). Isolation and characterization of starch from mature soybeans. *Cereal Chemistry, 55*, 661–670.

Woo, J.-W., Yoon, G.-S., & Kim, H.-S. (1985). Physicochemical properties of yullmoo (*Coix lacryma-jobi* var. mayuen stapf.) and yeomjoo (*Coix lachryma-jobi* L.) starches. *Journal of Korean Agricultural Chemical Society, 28*, 19–27.

Wurzburg, O. B. (1986). Converted starches. In O. B. Wurzburg (Ed.), *Modified starch: Properties and uses* (pp. 3–40). Boca Raton, FL: CRC Press.

Xie, X., & Liu, Q. (2004). Development and physicochemical characterization of new resistant citrate starch from different corn starches. *Starch/Stärke, 56*, 364–370.

Xie, X., Liu, Q., & Cui, S. W. (2006). Studies on the granular structure of resistant starches (type 4) from normal, high amylose and waxy corn starch citrates. *Food Research International, 39*, 332–341.

Zobel, H. F. (1964). X-ray analysis of starch granules. In R. L. Whistler (Ed.), *Methods in carbohydrate chemistry, Vol. 4. Starch* (pp. 109–113). New York: Academic Press.